ELSEVIER

SCIENCE DIRECT

Solid State Sciences 6 (2004) 1375–1380

Solid State Sciences

www.elsevier.com/locate/ssscie

A mixed cation nickel diphosphate with a layered intergrowth structure: synthesis, structural and magnetic characterization of $Na(NH_4)[Ni_3(P_2O_7)_2(H_2O)_2]$

Wei Liu [a], Xin Xin Yang [a], Hao Hong Chen [a], Ya Xi Huang [b], Walter Schnelle [b], Jing Tai Zhao [a,*]

[a] *State Key Laboratory of High Performance Ceramics and Superfine Microstructure, Shanghai Institute of Ceramics, Chinese Academy of Science, Shanghai, 200050, China*

[b] *Max-Planck-Institut für Chemische Physik fester Stoffe, Nöthnitzer Str. 40, 01178 Dresden, Germany*

Received 8 June 2004; accepted 27 July 2004

Available online 25 September 2004

Abstract

A nickel diphosphate with mixed cations, $Na(NH_4)[Ni_3(P_2O_7)_2(H_2O)_2]$ with a layered structure has been synthesized under hydrothermal conditions for the first time and characterized by single crystal X-ray diffraction, IR spectroscope and magnetization measurements. The structure consists of *cis*- and *trans*-edge sharing NiO_6 octahedral chains linked via P_2O_7 units to $[Ni_3P_4O_{16}]^{2-}$ layers. The ammonium and sodium cations are alternately located in the interlayer spaces. The mixed cations play an important role in the structural formation of this layered compound, leading to a new layer-stacking variant. The magnetic susceptibility obeys a Curie–Weiss law with μ_{eff} of 3.32 μ_B, showing the Ni^{2+} character and weak antiferromagnetic interactions.

Keywords: Hydrothermal synthesis; Layered structure; Diphosphate; Crystal structure

1. Introduction

Layered metal phosphates have been extensively studied during the past decades for their notable magnetism, ion-exchange ability, interlayer ionic mobility and intercalation [1–3]. For example, intercalation studies showed that the insertion of Cu^{2+} in the layered phosphate, $HNiPO_4{\cdot}H_2O$, produced interesting changes on the magnetic behavior of the matrix phases, an aspect which could be important for applications of the materials [4]. In this context, it is desirable to synthesize more materials with layered structures. Considerable efforts, especially hydrothermal techniques ($T < 700$ K, erogenous pressure) have yielded a variety of two-dimensional metal phosphates and the metals include gallium, indium, titanium, iron, tin, vanadium, cobalt, nickel, zinc [5–19]. In these systems, only three Ni-compounds, namely $NH_4NiPO_4{\cdot}H_2O$, $PbNi_3(P_2O_7)_2$, $Na(H_3O)_2Ni_4(OH)_4(HPO_4)_3(H_2PO_4)$ are reported in the literature [20–22].

The cations have an important role in the structural formation of phosphate and related materials. For example, different structural types of indium borophosphates can be obtained by introducing various cations [23–26]. More attention, therefore, is focused on the mixed cation compounds since they offer more varieties of size, shape and electrovalence. To date, mixed cation compounds are still rare. Here we report the hydrothermal synthesis, structural and magnetic characterization of a new mixed cation nickel diphosphate with a layered structure, $Na(NH_4)[Ni_3(P_2O_7)_2(H_2O)_2]$, **1**.

* Corresponding author.
E-mail address: jtzhao@mail.sic.ac.cn (J.T. Zhao).

1293-2558/$ – see front matter
doi:10.1016/j.solidstatesciences.2004.07.035

2. Experimental

2.1. Synthesis and characterization

Initially, the title compound was synthesized in an attempt to make imidazole-templated transition metal borophosphates. In a typical synthesis, thus, $NiCl_2{\cdot}6H_2O$ (2.38 g), $Na_2B_4O_7{\cdot}10H_2O$ (3.81 g), imidazole (2.04 g) and deionized water (15 mL) were mixed in the molar ratio 1:1:3:667. An amount of 5 mL of H_3PO_4 (85 wt%) was gradually added to adjust the pH at 1.0. The solution was then transferred to a Teflon-lined stainless steel autoclave and was heated at 523 K for 3 days under autogenetic pressure. The products were not a pure phase. Besides some dark viscous impurity, which should be the carbon residue resulting from the decomposition of organic molecules at high temperature, there exist two types of crystals: light green transparent hexagonal bipyramidal crystals and yellow plate-like crystals. The reaction products were separated by vacuum filtration, washed thoroughly with deionized water and ethanol to get rid of impurities, and finally dried in air. The two types of crystals were then separated by hand. All peaks of the X-ray diffraction pattern for the bipyramidal crystals are consistent with those of a known nickel borophosphate, $Na(H_2O)_2[NiBP_2O_8]{\cdot}H_2O$ [27], while the pattern of the plate-like crystals indicates that it is a new material. Subsequently, we obtain the pure phase of **1** successfully by using the NaCl (0.58 g) and $NH_4H_2PO_4$ (1.15 g) instead of $Na_2B_4O_7{\cdot}10H_2O$ and imidazole at 447 K for 5 days, but all other conditions are kept constant. The yield is 75% based on $NiCl{\cdot}6H_2O$.

The obtained crystals were initially examined by powder X-ray diffraction, using a Rigaku D/max 2550V diffractometer with Cu-Kα radiation, to establish phase identity. The patterns were entirely consistent with those calculated from the structure determined by single crystal X-ray diffraction. Scanning electron microscopy (SEM) and energy dispersive spectroscopy (EDS) were done on an EPMA-8705QH_2 electron microscope equipped with a LINKS ISIS. EDS analysis gives a Ni/P ratio of 2.92:4 (calcd. 3:4). Ni, P and Na contents were analyzed using ICP-AES (Varian Vista, radial observation), while a hot extraction method was applied for nitrogen (Leco CHNS-932), (obs.(esd)/calcd.) mass (%): Ni, 29.21/29.30; P, 20.47/20.63; Na, 3.78/3.83; N, 2.87/2.99. The results are in agreement with the formula of **1** found from the single crystal analysis.

An infrared spectrum was collected on a Digilab-FTS-80 spectrophotometer using KBr pellets of the samples. The IR spectrum showed features consistent with the presence of –OH and NH_4^+ groups in **1**. Thus, a broad band observed at 3425 and 1641 cm^{-1} corresponds to the stretching and bending vibrations of O–H. The peaks at 3233 and 1451 cm^{-1} were attributed to the stretching and bending vibrations of the N–H groups. Peaks observed in the region 1128–943 cm^{-1} are associated with terminal stretching modes of the P_2O_7 unit. Thermogravimetric analyses and differential scanning calorimetry (TGA and DSC) were performed using a STA-409PC/4/H LUXX DSC-TGA instrument at a heating rate of 10 K min^{-1} in a flow of nitrogen atmosphere from room temperature to 1273 K and showed a near featureless total weight loss of 9.1% occurring over the very broad range 543–833 K, corresponding to the removal of ammonia and water molecules in the structure.

Table 1
Crystallographic data for $Na(NH_4)[Ni_3(P_2O_7)_2(H_2O)_2]$

Formula weight	601.07
Wavelength (Å)	0.71073
Temperature (K)	293
Crystal system	Monoclinic
Space group	$C2/c$
a (Å)	18.989(4)
b (Å)	7.9758(16)
c (Å)	9.1112(18)
β (deg)	108.39(3)
V (Å^3)	1309.4(5)
Z	4
D_x (g cm^{-3})	3.049
μ (mm^{-1})	4.891
$F(000)$	1192
θ range (deg)	2.79–27.12
Total data collected	3191
S	0.965
R_1[a], wR_2[b]	0.0267, 0.0601
R_1, wR_2 (all data)	0.0305, 0.0614
Largest diff. peak and hole (e Å^{-3})	0.552, −0.462

[a] $R_1 = S||F_o| - |F_c||/\sum|F_o|$.
[b] $wR_2 = \{\sum[w(F_o^2 - F_c^2)^2]/\sum[w(F_o^2)^2]\}^{1/2}$, where $w = 1/[\sigma^2(F_o^2) + (0.0302P)^2 + 5.74P]$ with $P = (F_o^2 + F_c^2)/3$.

2.2. Determination of crystal structure

Crystals from the title compound were selected under a polarizing microscope, glued to a thin glass fiber with cyanoacrylate (superglue) adhesive. A suitable one of them was chosen ($0.50 \times 0.20 \times 0.05$ mm^3) and data sets were collected on a Nonius Kappa CCD diffractometer (Mo-Kα radiation, $\lambda = 0.71073$ Å). The data were corrected for absorption using the SADABS program [28]. The structures were solved by direct methods and refined against $|F^2|$ with the aid of the SHELXTL-PLUS package [29]. All hydrogen positions were located from the Fourier map but were refined as riding in the final refinement. Additional information about the data collection and structure refinement is presented in Table 1 while atomic coordinates and displacement parameters, selected distances and angles are listed in Tables 2 and 3, respectively.

3. Results and discussion

3.1. Description of the structure

The structure consists of $[Ni_3P_4O_{16}]^{2-}$ layers with ammonium and sodium cations occupying the interlayer spaces,

Table 2
Atomic coordinates ($\times 10^4$) and equivalent isotropic displacement parameters ($Å^2 \times 10^3$) for $Na(NH_4)[Ni_3(P_2O_7)_2(H_2O)_2]$

Atom	X	Y	Z	U_{eq}[a]
Ni(1)	3151(1)	1116(1)	5675(1)	10(1)
Ni(2)	2500	−2500	5000	10(1)
P(1)	1008(1)	−3152(1)	5868(1)	10(1)
P(2)	1995(1)	−479(1)	7422(1)	9(1)
Na(1)	5000	−387(2)	7500	18(1)
O(1)	3858(2)	2417(3)	4825(3)	17(1)
O(2)	3171(1)	−3798(2)	7033(2)	12(1)
O(3)	2451(1)	−447(2)	6321(2)	10(1)
O(4)	1198(1)	−1218(2)	6392(2)	11(1)
O(5)	3992(1)	910(3)	7693(2)	14(1)
O(6)	255(1)	−3038(3)	4682(2)	16(1)
O(7)	3394(1)	−1241(2)	4792(2)	12(1)
O(8)	2300(1)	1732(3)	3721(2)	11(1)
N(1)	0	−279(7)	2500	48(2)
H(1)	3671(1)	2731(1)	3901(1)	50
H(2)	4281(1)	2171(1)	4891(1)	50
H(3)	361(1)	401(1)	2751(1)	50
H(4)	−41(1)	−1081(1)	1631(1)	50

[a] U_{eq} is defined as one-third of the trace of the orthogonalized U_{ij} tensor.

as shown in Fig. 1. The asymmetric unit contains two crystallographically distinct nickel atoms and two independent phosphorus atoms. Both nickel atoms are coordinated by six oxygen neighbors (Ni–O = 2.026(5)–2.151(5) Å), so that slightly distorted octahedra are formed. Two phosphorous atoms are tetrahedrally coordinated linked through O(4) to form a P_2O_7 group. The pyrophosphate group acts as a bidentate ligand to Ni(1), thus producing a fairly bent P_2O_7 group (∠P(1)–O(4)–P(2) = 126.64(12)°) and resulting in the distortion of PO_4 tetrahedra (P–O = 1.621(3)–1.498(7) Å). There also exist three 3-coordinated oxygen atoms (O(3), O(7), O(8)) (see Fig. 2), linking nickel and phosphorous atoms to three-membered rings (Ni_2PO_3 or NiP_2O_7).

The structure of $[Ni_3P_4O_{16}]^{2-}$ layers are constructed from edge-sharing NiO_6 octahedral chains and pyrophosphate groups. The Ni(2)O_6 octahedra share *trans*-edges with two Ni(1)O_6 octahedra, while the Ni(1)O_6 octahedra share *cis*- and *trans*-edge with neighboring Ni(1)O_6 and Ni(2)O_6 octahedra forming an one-dimensional "zigzag" chain along the *b* axis (Fig. 3a). The P_2O_7 units act as bidentate ligands bonding with Ni(1) and N(2) via O(5), O(8), O(2) and Ni(2) of the neighboring chain via O(3), O(7), respectively, to an infinite layer, as shown in Fig. 3b. The remaining oxygen, O(6) of the P_2O_7 group is coordinated solely to P(1) and points into the interlayer space. The interspaces of the layers are separated by P_2O_7 groups into alternative large and small semi-enclosed spaces, where ammonium and sodium cations are located, respectively (see Fig. 1).

Similar two-dimensional topological structure can be also found in the previously reported diphosphates $PbNi_3(P_2O_7)_2$ [22], $K_3Co_3(P_2O_7)\cdot H_2O$ [30] and $(NH_4)_2[Mn_3(P_2O_7)_2(H_2O)_2]$ [31]. Compared to these layered cobalt and manganese diphosphates, the title compound reported here is different in several aspects. The crucial distinguishing point is that **1** has a different layer stacking, giving rise to other essential structural differences such as different space group and crystal lattice. Thus, **1** possesses crystallographical a new structure type. In order to illuminate distinctly the different layer-stacking between **1** and $PbNi_3(P_2O_7)_2$, $(NH_4)_2[Mn_3(P_2O_7)_2(H_2O)_2]$ or $K_3Co_3(P_2O_7)\cdot H_2O$, we replace the layers by a simple motif. Thus, as shown in Fig. 4(a), we choose a trapezium by linking of four neighboring P atoms along the NiO_6 octahedral chains as the basic unit, and hence the whole layer can be represented as a motif built from edge-sharing basic units. The corresponding structural sketches of $K_3Co_3(P_2O_7)\cdot H_2O$ (having the same layer-stacking with $PbNi(P_2O_7)_2$ and $(NH_4)_2[Mn_3(P_2O_7)_2(H_2O)_2]$) and **1** with cations are shown in Fig. 4(b) and 4(c), respectively. It can be shown apparently that the layers are arranged in the "*bbbb*" parallel in $K_3Co_3(P_2O_7)\cdot H_2O$ (see Fig. 4(b)), while **1** has

Table 3
Selected bond distances (Å) and angles (deg) for $Na(NH_4)[Ni_3(P_2O_7)_2(H_2O)_2]$

Ni(1)–O(5)	2.027(2)	P(1)–O(7)[b]	1.522(2)
Ni(1)–O(1)	2.035(2)	P(1)–O(4)	1.620(2)
Ni(1)–O(3)	2.040(2)	P(2)–O(2)[d]	1.498(2)
Ni(1)–O(8)	2.052(2)	P(2)–O(8)[e]	1.516(2)
Ni(1)–O(8)[a]	2.069(2)	P(2)–O(3)	1.517(2)
Ni(1)–O(7)	2.151(2)	P(2)–O(4)	1.620(2)
Ni(2)–O(7)	2.032(2)	Na(1)–O(5)	2.231(2)
Ni(2)–O(7)[b]	2.032(2)	Na(1)–O(5)[f]	2.231(2)
Ni(2)–O(3)[b]	2.051(2)	Na(1)–O(6)[b]	2.271(2)
Ni(2)–O(3)	2.051(2)	Na(1)–O(6)[g]	2.271(2)
Ni(2)–O(2)[b]	2.153(2)	O(1)–H(1)	0.84(5)
Ni(2)–O(2)	2.153(2)	O(1)–H(2)	0.81(5)
P(1)–O(6)	1.498(2)	N(1)–H(3)	0.85(4)
P(1)–O(5)[c]	1.509(2)	N(1)–H(4)	1.01(4)
O(5)–Ni(1)–O(1)	87.76(10)	O(3)–Ni(2)–O(2)	88.12(9)
O(5)–Ni(1)–O(3)	95.00(9)	O(3)[b]–Ni(2)–O(2)	89.82(8)
O(1)–Ni(1)–O(3)	172.05(9)	O(3)[b]–Ni(2)–O(2)	90.18(8)
O(5)–Ni(1)–O(8)	170.65(8)	O(7)–Ni(2)–O(2)[b]	91.88(9)
O(1)–Ni(1)–O(8)	88.91(10)	O(7)[b]–Ni(2)–O(2)[b]	88.12(9)
O(3)–Ni(1)–O(8)	89.47(8)	O(3)–Ni(2)–O(2)[b]	90.18(8)
O(5)–Ni(1)–O(8)[a]	95.73(8)	O(3)[b]–Ni(2)–O(2)[b]	89.82(8)
O(1)–Ni(1)–O(8)[a]	93.19(9)	O(2)–Ni(2)–O(2)[b]	180.0
O(3)–Ni(1)–O(8)[a]	93.94(8)	O(6)–P(1)–O(5)[c]	113.30(13)
O(8)–Ni(1)–O(2)[a]	75.73(9)	O(6)–P(1)–O(7)[b]	113.28(13)
O(5)–Ni(1)–O(7)	93.85(8)	O(5)[c]–P(1)–O(7)[b]	112.93(13)
O(1)–Ni(1)–O(7)	93.36(9)	O(6)–P(1)–O(4)	103.14(12)
O(3)–Ni(1)–O(7)	79.04(8)	O(5)[c]–P(1)–O(4)	106.07(12)
O(8)–Ni(1)–O(7)	95.07(8)	O(7)[b]–P(1)–O(4)	107.14(12)
O(7)[b]–Ni(2)–O(7)	180.00(7)	O(2)[d]–P(2)–O(8)[e]	113.52(12)
O(7)[b]–Ni(2)–O(3)[b]	81.61(8)	O(2)[d]–P(2)–O(3)	115.36(12)
O(7)–Ni(2)–O(3)[b]	98.41(8)	O(8)[e]–P(2)–O(3)[c]	111.71(12)
O(7)[b]–Ni(2)–O(3)	98.41(8)	O(2)[d]–P(2)–O(4)	105.17(12)
O(7)–Ni(2)–O(3)	81.59(8)	O(8)[e]–P(2)–O(4)	105.58(12)
O(7)–Ni(2)–O(2)	91.88(9)	O(3)–P(2)–O(4)	104.30(11)
O(3)[b]–Ni(2)–O(3)	180.00(12)	H(3)–N(1)–H(4)	118(4)

[a] $-x+1/2, -y+1/2, -z+1$; [b] $-x+1/2, -y-1/2, -z+1$; [c] $-x+1/2, y-1/2, -z+3/2$; [d] $-x+1/2, y+1/2, -z+3/2$; [e] $x, -y, z+1/2$; [f] $-x+1, y, -z+3/2$; [g] $x+1/2, -y-1/2, z+1/2$.

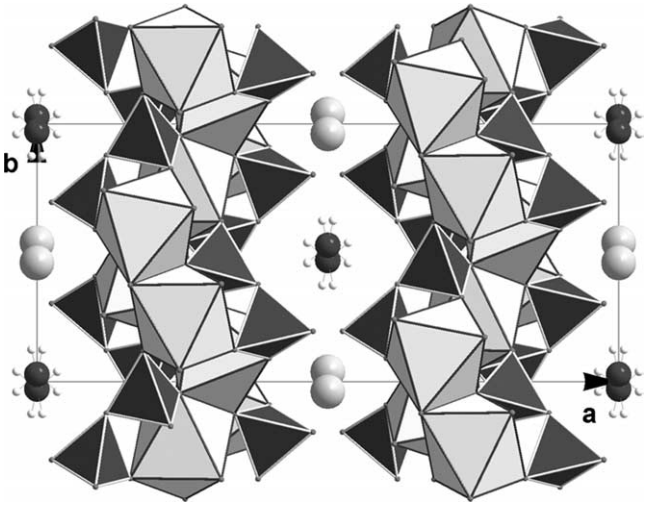

Fig. 1. Polyhedral view of $Na(NH_4)[Ni_3(P_2O_7)_2(H_2O)_2]$ along the *c* axis showing the $[Ni_3P_4O_{16}]^{2-}$ layers with ammonium and sodium cations occupying the interlayer space (NiO_6 octahedra, light-grey; PO_4 tetrahedra, dark-grey; Na cations, light-grey sphere; NH_4^+ cations, dark sphere and little light-grey sphere).

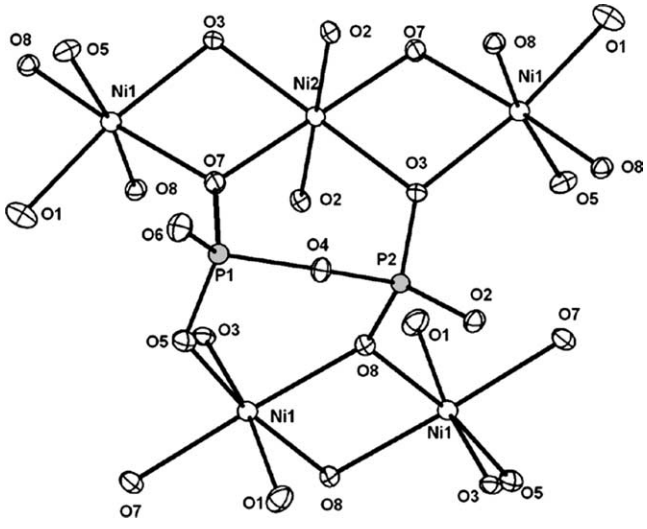

Fig. 2. Thermal ellipsoid plot (50% probability) and atomic labeling scheme for the $[Ni_3P_4O_{16}]^{2-}$ layers, showing the 3-coordinated oxygen atoms and the P_2O_7 unit.

the symmetrical arrangement of layers in the form of "*bdbd*" (see Fig. 4(c)). This layer-stacking changement in the structure may result from the effect of the mixed cations. With mixed cations in a structure the individual cations can occupy different spaces. This provides the compound more choices such as changing the arrangement of layers to obtain different spaces for cations with various sizes. As a result, **1** adopts the symmetrical arrangement of layers in the form of "*bdbd*" to create various spaces for large cations NH_4^+ and small cations Na^+, respectively, which indicates that the mixed cations play an important role on the structural formation of **1**, leading to a new layer stacking variants.

Ammonium and sodium cations occupy the interlamellar spaces between the layers and satisfy the charge balance.

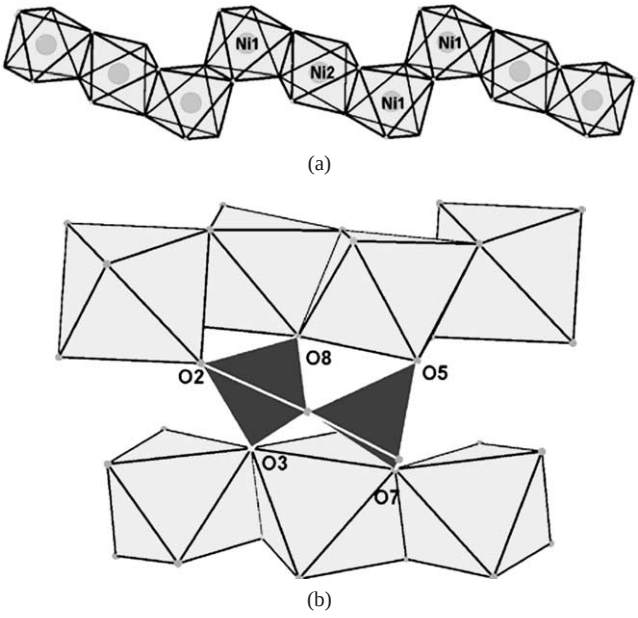

Fig. 3. (a) Polyhedral view of the one-dimensional "zigzag" chain along the *b* axis (b). View of single $[Ni_3P_4O_{16}]^{2-}$ layer showing the NiO_6 chains connecting by the P_2O_7 units (NiO_6 octahedra, light-grey; PO_4 tetrahedra, dark-grey).

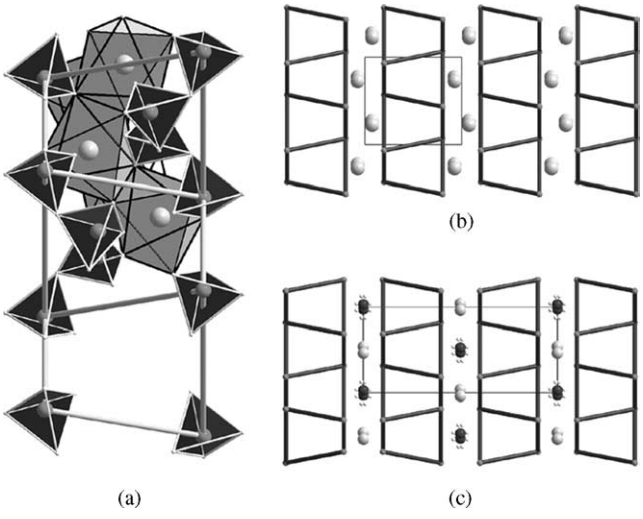

Fig. 4. (a) The model of the layer with part of polyhedra (NiO_6 octahedron, grey; PO_4 tetrahedron, dark). (b) The structural diagrammatic sketches of $K_3Co_3(P_2O_7)\cdot H_2O$ with K^+ cations (light-grey sphere). (c) The structural diagrammatic sketches of $Na(NH_4)[Ni_3(P_2O_7)_2(H_2O)_2]$ with mixed cations (Na^+, light-grey sphere; NH_4^+, dark sphere with small light-grey sphere).

Nitrogen atoms are hydrogen bonded to the terminal oxygen atom from P_2O_7 units via N–H...O (N(1)–H(4)...O(6) = 1.81(8) Å), while the terminal oxygen of P_2O_7 group also bonds with the oxygen atom in $O(1)H_2$ group of the adjacent layer via hydrogen bonds (O(6)...H(2) = 1.93(2) Å). Furthermore, $O(1)H_2$ group interacts also with O(2) of the same layer via N–H...O (O(1)–H(1)...O(2) = 1.89(2) Å). All of hydrogen bonds constitute a hydrogen-bond-net surround-

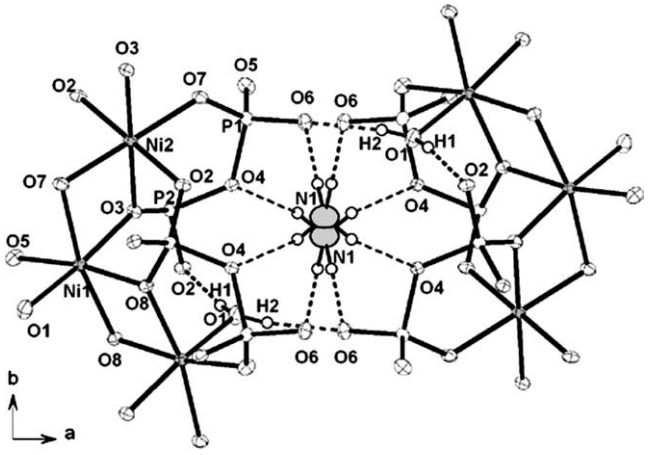

Fig. 5. The hydrogen-bond-net surrounding and fixing the inorganic layers to a whole open-framework (N, large grey spheres; H, little while spheres; the dot lines are hydrogen bonds).

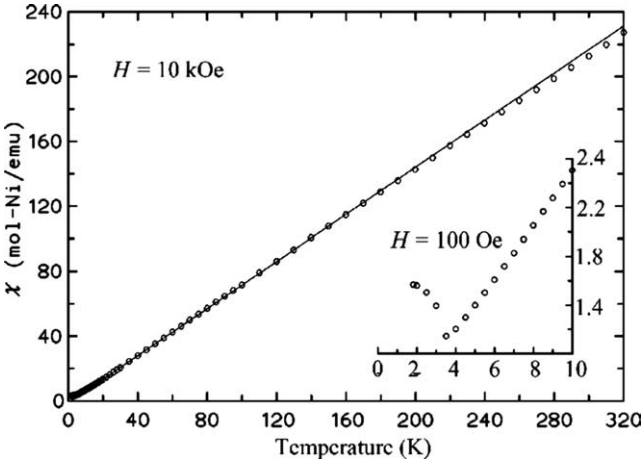

Fig. 6. The temperature dependence of the inverse magnetic susceptibility of **1** with $H = 10$ kOe. The inset shows data for $H = 100$ Oe at low temperatures.

ing and fixing the inorganic anions to an open-framework, as shown in Fig. 5.

3.2. Magnetic characterization

The magnetization was measured with a SQUID magnetometer (Quantum-Design, MPMS XL-7) in the temperature range 1.8–320 K. The temperature dependence of the magnetic susceptibility $\chi = M/H$ of compound **1** was investigated in various magnetic fields. The susceptibility for $H = 10$ kOe (Fig. 6) obeys approximately a Curie-law over almost the whole temperature range. From a nonlinear fit of a Curie–Weiss law $\chi = C/(T - \Theta)$ to the data in the temperature range (20–320 K), a Weiss temperature $\Theta = -1.47(3)$ K (antiferromagnetic) can be obtained, demonstrating that magnetic interactions are weak. The effective magnetic moment μ_{eff} per Ni obtained from this fit is 3.32 μ_B, a value well within the range reported for octahedrally coordinated Ni^{2+} ions (2.9–3.4 μ_B) [32,33]. The g-factor calculates to 2.348. A linear fit of $1/\chi$ in the same temperature range yields $\mu_{\text{eff}}/\text{Ni} = 3.35\mu_B$ and $\Theta = -0.12$ K. A weak cusp in $\chi(T)$ for $H = 100$ Oe at 3.5(4) K and a decrease of χ below this temperature indicates an antiferromagnetic ordering of the Ni moments (Fig. 6, inset). Considering the structural features exhibited by this nickel diphosphate, the magnetic interactions between chains are comparatively weak since the NiO_6 octahedra chains are separated from each other by P_2O_7 groups with a distance of 2.53 Å. Within a chain, the Ni...Ni distances are too large to allow significant direct Ni–Ni magnetic exchange (Ni(1)...Ni(1) = 3.252 Å, Ni(1)...Ni(2) = 3.121 Å). Thus, another pathway implies the magnetic coupling through –Ni(2)O_6–Ni(1)O_6–Ni(1)O_6– metallic chains in the [010] direction, which are formed by edge sharing between MO_6 octahedra. This exchange pathway would produce antiferromagnetic coupling in the sub-network of transitional metal polyhedra, which is consistent with the antiferromagnetic ordering observed in the title compound at lower temperature.

4. Conclusion

A mixed cations layered nickel diphosphate, $Na(NH_4)[Ni_3(P_2O_7)_2(H_2O)_2]$, has been hydrothermally synthesized at 523 K in presence of imidazole. The crystal structure is characterized by the polyhedral layers $[Ni_3P_4O_{16}]^{2-}$, which are closely related to those found in $(NH_4)_2[Mn_3(P_2O_7)_2(H_2O)_2]$ and $K_3Co_3(P_2O_7)\cdot H_2O$, and ammonium and sodium cations occupying the interlayer spaces. However, **1** has a different layer stacking compared to those layered cobalt and manganese diphosphates, which results from the existence of mixed cations. Thus, it indicates that mixed cations have an important effect on the structural formation for this layered compound, an aspect, which deserves attention in the synthesis of novel, layered compounds.

Supplementary material

The supplementary material has been sent to the Fachinformationzentrum Karlsruhe, Abt. PROKA, 76344 Eggenstein-Leopoldshafen, Germany, as supplementary material and can be obtained by contacting the FIZ (CSD 414111).

Acknowledgements

This work was supported by the Fund for Distinguished Young Scholars (20025101) and Key Project (50332050) from the NNSF of China, State “863” Project (2002AA324070) and fund of Shanghai Optical Science and Technology (011161015).

References

[1] S.L. Suib, Chem. Rev. 93 (1993) 803.

[2] A.K. Cheetham, G. Férey, T. Loiseau, Angew. Chem., Int. Ed. 38 (1999) 3268.
[3] A.M. Chippindale, F.O.M. Gaslain, A.R. Cowley, A.V. Powell, J. Mater. Chem. A 11 (2001) 3172.
[4] A. Goñi, L. Lezama, J.L. Pizarro, J. Escobal, M.I. Arriortua, T. Rojo, Chem. Mater. 11 (1999) 1752.
[5] M.P. Attfield, A.K. Cheetham, S. Natarajan, Mater. Res. Bull. 35 (2000) 1007.
[6] C. Paulet, T. Loiseau, G. Férey, J. Mater. Chem. 10 (2000) 1225.
[7] S. Natarajan, A.K. Cheetham, J. Solid State Chem. 140 (1998) 435.
[8] J. Do, R.P. Bontchev, J.A. Jacobson, Inorg. Chem. 39 (2000) 3230.
[9] S. Ekambaram, S.C. Sevov, J. Mater. Chem. 10 (2000) 2522.
[10] Y.N. Zhao, G.S. Zhu, X.L. Jiao, W. Liu, W.Q. Pang, J. Mater. Chem. 10 (2000) 463.
[11] K.H. Lii, Y.F. Huang, Inorg. Chem. 38 (1999) 1348.
[12] X.Q. Wang, L.M. Liu, H.D. Cheng, K. Ross, A.J. Jacobson, J. Mater. Chem. 10 (2000) 1203.
[13] S.Y. Mao, Y.X. Huang, Z.B. Wei, J.X. Mi, Z.L. Huang, J.T. Zhao, J. Solid State Chem. 149 (2000) 292.
[14] Y.P. Chiang, H.M. Kao, K.H. Lii, J. Solid State Chem. 162 (2001) 168.
[15] B.G. Shpeizer, X. Ouyang, J.M. Heising, A. Clearfield, Chem. Mater. 13 (2001) 2288.
[16] W. Liu, Y.L. Liu, Z. Shi, W.Q. Pang, J. Mater. Chem. 10 (2000) 1451.
[17] C. du Peloux, A. Dolbecq, P. Mialane, J. Marrot, E. Rivière, F. Sécheresse, Angew. Chem., Int. Ed. 40 (2001) 2455.
[18] S. Fernández, J.L. Mesa, J.L. Pizarro, L. Lezama, M.I. Arriortua, R. Olazcuaga, T. Rojo, Chem. Mater. 12 (2000) 2092.
[19] Q.M. Gao, N. Guillou, M. Nogues, A.K. Cheetham, G. Ferey, Chem. Mater. 11 (1999) 2937.
[20] A. Goñi, J.L. Pizarro, L.M. Lezama, G.E. Barberis, M.I. Arriortua, T. Rojo, J. Mater. Chem. 6 (1996) 421.
[21] N. Hamanaka, H. Imoto, Inorg. Chem. 37 (1998) 5844.
[22] V.V. Krasnikov, Z.A. Konstant, V.K. Bel'skii, Izv. Akad. Nauk SSSR, Neorg. Mater. 21 (1985) 1560.
[23] Y.X. Huang, J.X. Mi, S.Y. Mao, Z.B. Wei, J.T. Zhao, R. Kniep, Z. Kristallogr. NCS 217 (2002) 7.
[24] S.Y. Mao, M.R. Li, Y.X. Huang, J.X. Mi, Z.B. Wei, J.T. Zhao, R. Kniep, Z. Kristallogr. NCS 217 (2002) 3.
[25] J.X. Mi, M.R. Li, S.Y. Mao, Y.X. Huang, Z.B. Wei, J.T. Zhao, R. Kniep, Z. Kristallogr. NCS 217 (2002) 5.
[26] Y.X. Huang, J.T. Zhao, J.X. Mi, H. Borrmann, R. Kniep, Z. Kristallogr. NCS 217 (2002) 163.
[27] I. Boy, G. Schäfer, R. Kniep, Z. Kristallogr. NCS 216 (2001) 11.
[28] (a) R.H. Blessing, Acta Crystallogr. A 51 (1995) 33;
(b) SADABS, Area-detector absorption correction, Bruker-AXS, Madison, WI, 1996.
[29] G.M. Sheldrick, SHELXL-97, Program for refining crystal structures, University of Göttingen, Germany, 1997.
[30] P. Lightfoot, A.K. Cheetham, J. Solid State Chem. 85 (1990) 275.
[31] A.M. Chippindale, F.O.M. Gaslain, A.D. Bond, A.V. Powell, J. Mater. Chem. 13 (2003) 1950.
[32] F. Sanz, C. Parada, J.M. Rojo, C. Ruíz-Valero, Chem. Mater. 13 (2001) 1334.
[33] T. Yoshida, T. Suzuki, K. Kanamori, S. Kaizaki, Inorg. Chem. 38 (1999) 5926.